Egypt. J. Bot., **Vol. 63,** No. 3, pp. 765-786 (2023)

Egyptian Journal of Botany
http://ejbo.journals.ekb.eg/

Pleotropic Roles of Biosynthesized Cerium Oxide Nanoparticles on Morphological, Physiological and Molecular Aspects on *Brassica napus*

Salma M. Awad[(1)#], Tahani A. Hathout[(1)], Samia M. El khallal[(1)], Khaled Y. Farroh[(2)]

[(1)]Botany Department, Faculty of Women for Arts, Science and Education, Ain Shams University, Cairo 11757, Egypt; [(2)]Nanotechnology and Advanced Material Central lab (NAMCL), Agricultural Research Center, Giza, Egypt.

THE AIM of this study was to determine how cerium dioxide nanoparticles (CeO_2 NPs) affect the growth and physiology of *Brassica napus* plants. CeO_2 NPs were biosynthesized using *Aloe Vera* extract and characterized using a UV-visible spectrophotometer, X-ray diffraction, Fourier transform infrared spectroscopy, Zeta potential, and particle size (DLS) as well as transmission electron microscopy. Following foliar treatment with 250, 500, and 1000ppm of CeO_2 NPs, the growth, and metabolism of *Brassica napus* were evaluated. Exposure to 500ppm CeO_2 NPs significantly enhanced morphological characteristics, antioxidant enzymes, phenol content, tocopherol, and chlorophyll content as well as carotenoid levels in *B. napus*. Assessment of oxidative stress in *B. napus* leaves treated with 500 CeO_2NPs showed high levels of super oxide anion radical ($o_2^{\cdot-}$) and hydrogen peroxide and low content of MDA, as well as inhibition in the activity of Lipoxygenase enzyme. Histochemical staining of *B. napus* leaves using nitro blue tetrazolium confirms the role of spraying of 500ppm of CeO_2 NPs in the accumulation of oxidative molecules in leaves. Gene expression assay for SOD and MT highlighted the role of CeO_2 NPs in the regulation of stress-related genes in tested plants. The changes in ultrastructure of *Brassica napus* leaves treated or untreated with 500ppm of CeO_2 NPs for two weeks were examined using a transmission electron microscope.

Keywords: *Brassica napus,* Cerium dioxide nanoparticles, Morphology, Oxidative stress.

Introduction

Family Brassicaceae includes *Brassica napus* (canola) plays an important role in the economy of many landowners in Europe. It produced green fuel that could be utilized for human consumption, pet feeding, chemical processing, and the pharmaceutical industry. Compared to crops like wheat and maize, oilseed rape was only domesticated to a limited extent. (Friedt & Snowdon, 2009), and canola has enormous economic importance for many farmers in Europe (Rafael et al., 2018).

Nanotechnology has become one of the most efficient and powerful techniques for battling stressful ecological events in plants as a result of advancements in diverse research fields. Nanoparticles can affect physiological functions, photosynthesis, and protection against oxidative enzymes in plants due to their exceptional total area, structure, and shape (Eldarier et al., 2020; Hafez & Fouad, 2020; Faizan et al., 2021). Due to various industrial circumstances connected with nanoparticles, people are concerned about their effects on human and envirmental health as a result of the extensive use of these molecules in many sectors (Lee et al., 2020).

The technical framework of research that explains the mechanisms of NPs is very important and has enable broad applications in plants (Sahoo et al., 2007). NPs have drawn the interest of numerous

[#]Corresponding author email: m.salma.awad@women.asu.edu.eg
ORCID ID: 0000-0002-9811-8896
Received 11/08/2022; Accepted 20/03/2023
DOI: 10.21608/ejbo.2023.155777.2097
Edited by: Dr. Mahmoud M.Y. Madany, Biology Department, College of Science, Taibah University, KSA.

research communities, owing to their unique properties such as large surface area of substance (Ejaz et al., 2018). On the other hand, because of the increased production of NPs for use in everyday products, contamination of ecosystems is a serious concern (Liu et al., 2021). Managing the distribution of NPs that are specially engineered according to our needs into the ecosystem has proven challenging due to growth of the nanomaterials industries and their usage (Sohail et al., 2022). Further research is required, as there is a severe lack of information on the ecological effects of NPs.

Cerium dioxide nanoparticles (CeO_2 NPs) have a variety of commercial, physiological, medicinal, and agronomic applications because of their remarkable electric, visual, and other beneficial properties (Cassee et al., 2011).

Cerium oxide nanoparticles are employed extensively in plant biology due to the antioxidant properties of these nanoparticles (Wang et al., 2013). They have been shown to lower excess ROS accumulation, improving plant responses to environmental stresses such as salt (Wang et al., 2013; Rossi et al., 2017), sunlight, and climate change (Rossi et al., 2017). Moreover, Wu et al. (2017) reveals that nanoparticles might modify the functions of transmembrane proteins associated with K^+ release to improve mesophyll K^+ storage and activate the transcription of the HKT1 gene to enhance shoot Na^+ exclusion, thereby enhancing plant drought tolerance. Many studies reported that CeO_2 NPs either reduce or intensify stress in plants depending on the dose (Prakash et al., 2021). Additionally, Khan et al. (2021) reported that CeO_2 NPs can regulate oxidative stress.

In the present study, foliar application of 250, 500, and 1000ppm of biosynthesized CeO_2 NPs to *B. napus* was used to determine various responses of its morphological, and physiological parameters as well as gene expression and ultrastructure examination reflecting the impact of CeO_2 NPs.

Materials and Methods

Synthesis of Cerium oxide nanoparticles

To prepare cerium oxide nanoparticles, we used the Cerium (III) nitrate hex hydrate, REacton®, 99.99%, (REO). Thermo scientific™ Stock Number: 11330, Lot Number G31U002 ($Ce(No_3)_3.6H_2O$), (MW 434.22g/mol), as the prime precursor and Aloe vera leaf extract as the stabilizing agent according to the method by Dutta et al. (2016).

Preparation of aloe vera leaf extract

About 30g fresh gel of *Aloe vera* were boiled in 100 ml deionized water for 1h and the pH was recorded at 5.36 before adding cerium nitrate hexahydrate.

Cerium nanoparticle synthesis

According to Dutta et al. (2016) with some modification, about 0.087g of cerium nitrate hexahydrate (10mM) was dissolve in 20mL of DI water then added to 140mL of DI water at an initial temperature 40°C pH 5, then stirred with a magnetic stirring until a homogeneous solution was formed. After 1min the *Aloe vera* extract about 20mL was added dropwise for 20min under magnetic stirring with the pH set at 6 adjusted by NaOH (30mM) and a temperature range of 50-60°C. After the pH was adjusted to 8 for 20min by NaOH then readjust finally at pH 7.5 with HCl (30mM), the solution was left under magnetic stirring for 48h Then centrifuge all at 5000rpm for 30min and the precipitate was dried in an oven at 60°C for 1h and finally reddish-brown powder of CeO_2-Nps was obtained and was detected using an Agilent 5100 Inductively Coupled Plasma – Optical Emission Spectrometer (ICP-OES) with Synchronous Vertical Dual View (SVDV) with the Agliant Vapor generation accessory VGA 77 to determine its concentration was 1.72% and also used for preparing the different concentration at (250,500,1000ppm), which was sonicated for 1min before using as foliar application later on.

Characterization of cerium oxide nanoparticle

The UV–Vis absorption spectrum was detected by with a scanning protocol at 200-900nm using a Jenway 7205 spectrophotometer. The structure and crystal size of cerium dioxide nanoparticles were detected by an X-ray diffraction (XRD) pattern using an EQUINOX™ 100 X-Ray diffractometer with a Cu-K_α wavelength of 1.5406 Å in the 2θ range 0°- 80°. To visualize the shape and size measurement of core particles, the TEM technique was used by JEOL1010 transmission electron microscope (TEM). The Fourier transform infrared spectroscopy (FTIR) spectra of samples were recorded in the range of 800–4000cm^{-1} using a Thermo-Fisher FTIR spectrometer. Particle size and zeta potential were detected using Zetasizer Nano ZS (Yu et al., 2021).

Foliar application of CeO_2 NPs on Brassica napus plants

Pot experiment:

B. napus seeds cultivar 1056 were obtained from the Agricultural Research Center, Ministry of Agriculture, Egypt. The experiment was conducted in the Botanical Garden for Research of the Botany Department Faculty of Women for Arts, Sciences and Education, Ain Shams University, Egypt. In this experiment, about 40 pots (30 cm depth and 30cm diameter) were prepared and divided into groups A, B, C and D (5 pots/group) and filled with about 10kg of clay soil.

*Brassica na*pus seeds were surface sterilized with sodium hypochlorite for 3min and then washed with deionized water. About 20 sterile seeds were sown and left to grow under natural conditions. Plants at seedling stage and after the emergence of two true leaves, foliar application was performed using different concentrations of aqueous suspension of CeO_2 NPs (250,500,1000ppm) every 48h for two weeks' intervals. Plants of group A were sprayed with water and left as a comparison sample, while plants of groups B, C, and D were sprayed with concentrations of 250, 500, and 1000ppm of CeO_2 NPs, respectively. The plants were thinned about 5 per pots and the pots were covered with plastic bags after spraying. In this experiment, aqueous suspension of CeO_2 NPs was freshly prepared after sonication for 1min (as mentioned before). A drop of Tween-20 has been added as a surfactant agent.

Whole Plants were harvested at 45 days of age (after 15 days of spraying), washed with water and used for the biomasses and morphological parameters measurements. Other samples were frozen at -80°C for further biochemical analysis.

Detection of cerium levels

Prior to metal determination, dry plant tissues (0.5g) were digested in 2mL of an acid (hydrochloric acid and Aqua regia in a ratio 1:3) solution and then adding 1mL of 30% H_2O_2 using Anton –Paar microwave digestion system (Multijwave PRO) according to standard method (APHA, 2017) and determination of metal ions such as cerium was conducted using an Agilent 5100 Inductively Coupled Plasma – Optical Emission Spectrometer (ICP-OES) with Synchronous Vertical Dual View (SVDV) with the Agliant Vapor generation accessory VGA 77. where all samples are in an acceptable matrix for consistent recovery of metals which are compatible with the analytical method (APHA, 2017). A calibration curve was constructed composed of using a blank and three standards from Merck (Germany). Precision of measurements was confirmed using external reference standard, and quality control samples from National Institute of Standards and Technology (NIST) (Bao et al., 2016; Farooq et al., 2022).

Morphological alterations

Root, and shoot length as well as fresh and dry weights were measured to detect morphological differences in control samples and after spraying 250, 500 and 1000ppm of CeO_2 NPs nanoparticles (Mohammadi et al., 2021).

Enzymatic assays

The activity of peroxidase (POD), superoxide dismutase (SOD), and catalase enzymes activities were assayed. First, 1g of leaf samples in liquid nitrogen for prevent proteolytic activity were added to phosphate buffer (pH 7.8, 100mM) and completely homogenized. The homogenized mixture was centrifuged (8000 x g) at 4°C for 15 min, and the supernatant was used for the determination of the following enzyme activities.

Superoxide dismutase (SOD, EC 1.15.1.1) activity was determined with the method of Zhang et al. (2008). The reaction mixture was contained of 50mM potassium phosphate buffer (pH 7.8), 13mM methionine, 75µL NBT, 2µL riboflavin, 0.1mM EDTA and 100µL of enzyme extract in a 3mL total volume then followed by keeping samples under a 15W fluorescent tube for 10min. Then all tubes were wrapped with aluminum foil. The solution containing the reaction mixture without light irradiation considered as a blank, while the complete reaction mixture without plant extracts used as a control. One unit of SOD activity was measured the amount of enzyme required to cause 50 % inhibition of the NBT reduction measured at 560 nm is expressed as (Unit min^{-1} g^{-1} FW).

Catalase (CAT, EC 1.11.1.6) activity, as described in Aebi & Lester (1984). 3mL reaction mixture containing 50 mM potassium phosphate buffer (pH 7.0), 2mM EDTA-Na_2, 10mM H_2O_2 and 100µL enzyme extract. for 1min at A240nm using (T80+UV–visible spectrophotometer). The catalase activity was assayed by using the extinction coefficient of 39.4mM^{-1} cm^{-1}. One

unit of catalase activity is expressed as (µmol H_2O_2 reduced min^{-1} g^{-1} FW).

Peroxidase (POD, EC1.11.1.7) activity was assayed by Zhou & Leul (1999). The 1mL of mixture contained 50 mM potassium phosphate buffer (pH 7.0), 0.4% H_2O_2, 1% guaiacol, and 100µL enzyme extract. The reaction was followed by recording the changes in Absorbance at 470 nm. POD expressed as (µmol tetra-guaiacol formed min $^{-1}g^{-1}$ FW) and its extinction coefficient (E) = 2.47mM^{-1} cm^{-1}. Lipoxygenase activity assay (LOX; EC 1.13.1 I. 12) LOX activity was measured according to method described by Axelrod et al. (1981). A 0.5g leaves ground to a fine powder was added to 5mL of acetate buffer (pH 5.0), and incubated in ice water for 15min, followed by centrifugation at 10,000 x g for 10min. The aliquot was used as a crude enzyme extract. Components of the reaction were incubated at 25°C in a water bath, 100µL linoleic acid, 100µL crude enzyme extract and 2.8mL phosphate buffer (pH 6.8). The absorbance was measured by UV spectrophotometer at 234nm. A LOX activity unit (U/g FW) was defined as the rate of absorbance change per minute. One unit (U) of LOX activity was described as 1µmol of lipid hydroperoxides formed per minute at 25°C.

Antioxidant compounds

About 680 µL distilled water, 50 µL extract and 2.5mL 1/10 dilution of Folin–Ciocalteu reagent were mixed and vortexed. After 2min, 2mL Na_2CO_3 7.5% was added and the mixture was incubated for 15min at 45°C, the absorbance was measured at 760nm. The concentration of total phenolic compounds (TPCs) was expressed as mg gallic acid equivalents (GAE) per g of fresh weight (FW), and then calculated using a standard curve for gallic acid (Javanmardi et al., 2003). Tocopherol content was estimated according to Backer et al. (1980), 1g of fresh leaves was grinded in mortar and add 5mL of a mixture consisting of petroleum ether and ethanol (2:1.6) v/v then the extract was centrifuged at 10.000 for 20min. The supernatant was prepared for tocopherol estimation, take 1mL of extract, 200µL of 2% 2, 2-dipyridal in ethanol was added, then finally add 200µL of ferric chloride mixed vigorously then kept at dark for 5min. The resulting red color was diluted with 4mL of D.W and then mixed well, the color resulted was measured at 520nm. Tocopherol content was calculated using a standard curve with a known amount of alpha-tocopherol.

Ascorbic acid levels were determined according Jagota & Dani (1982). Plants tissue about (0.2g) were homogenized in 0.8mL of 10% tricholoroacetic acid (TCA). After shaking well, the tubes keep in an ice bath for 5min followed by centrifuged at 3000g for 5min. For the estimation of AsA, used a 300µL of extract. The extract was diluted to 2.0mL using D.W, then add 200µL of 1N Folin reagent was added, and all tubes were shaken, then Incubate for 10min the absorbance was measured at 760nm. Standard curve was prepared using AsA.

Physiological parameters

Chlorophyll determination

Fresh leaves tissue (1g) from various treatments were ground in chilled 70% acetone (analytical grade) with 100mg of calcium carbonate, and the absorbance was recorded at 645, 663nm for chlorophyll A, B at 480nm for carotenoids using a UV-Visible+T80 spectrophotometer (Jakhar & Mukherjee, 2014), and calculated using the following equation:

Chlorophyll a: 12.7(A663) – 2.69(A645)

Chlorophyll b: 22.9(A645) – 4.68(A663)

Carotenoid: [A480 +(0.114(A663) -(0.638-A645)] ×V/1000×W

Carbohydrate determination

About 0.5g of dry leaves was taken into a boiling tube, and 5mL of 2.5N HCl was added. The solution was boiled in a water bath for 3h. Phenol–Sulfuric Acid method the colorimetric method described by Dubois et al. (1956) it's used to determine of the concentration of carbohydrates in aqueous solutions. A 2mL aliquot of a carbohydrate solution was mixed with 1mL of 5% aqueous solution of phenol in a test tube. A 5mL of concentrated sulfuric acid was added rapidly to the mixture (an exothermic reaction and orange color were observed.) After stand for10min, they are vortexes for 30sec and stand for 20min at room temperature for color development. Next, light absorption at 490nm was measured by a spectrophotometer. Blank was prepared in the same way, except that the 2mL aliquot of solution was replaced by distilled water. A standard curve was prepared using glucose from 0 - 100µg mL^{-1}.and measure at a wavelength of 490nm. The carbohydrate rate was expressed as µg g^{-1} FW.

Lipid peroxidation assay

Lipid peroxidation was estimated by measuring

the amount of TBARS as previously described (Liu et al., 2007). About 0.5g leaves was ground in mortar with 0.25 % 2-thiobarbituric acid (TBA) in 10% TCA. The mixture was heated at 95°C for 30min, then, quickly cooled in an ice bath and centrifuged at 10 000g for 10min. The absorbance of the supernatant was recorded at 532nm and 600nm which corrected for unspecific turbidity by subtracting. Lipid peroxides concentration was together with modified protein were calculated in terms of TBARS amount using an extinction coefficient of $155mM^{-1}$ cm^{-1} and expressed as n mol g^{r} fresh weight**.** Hydrogen peroxide **(**H_2O_2) was determined by method of Fortunato et al. (2010), fresh leaves tissue (0.5g) from each treatment group) ground in 5mL 0.1 % (v/v) TCA solution on ice immediately. The suspension was then transferred to a 15mL centrifuge tube and centrifuged at 4000g for 20min at 4°C, an aliquot (0.5mL) of the supernatant mixed with 0.5mL of 10mM KH_2PO_4 solution (pH 7) and 1mL of 1M KI solution for measurement. The absorbance was measured using T80+UV/Vis spectrophotometer at 390nm, H_2O_2 was used as standard curve and. H_2O_2 content expressed as µmol H_2O_2 per g Tissue. The quantification of superoxide can also be determined as described previously by Ramel et al. (2009). Stained plant tissue was grind to a fine powder and dissolved in 2M KOH-DMSO (1/1.16) (v/v) after that centrifugation at 12000g for 10min. The aliquot was measured at 630nm in the UV spectrophotometer and the values were compared with the standard curve prepared using NBT prepared in the KOH-DMSO mix.

Staining of leaves

The detection of super oxides in plants have been reported by NBT histochemical methods (Doke et al., 1983; Jabs et al., 1996). The plant tissue under stress were immersed in staining solution including NBT 0.1%, 50mM potassium phosphate (pH 6.4) and 10mM sodium azide. Then, samples were kept under illuminate for 20min and then rinsed with 95% ethanol to get rid of the chlorophyll pigments. Blue precipitates appear as NBT reacts with superoxide anion, Cameras were used to take pictures of NBT colored leaves.

Molecular studies

Total RNA was extracted from approximately 100 mg of leaves by Trizol protocol. The synthesized cDNA from control and leaves sprayed with 500 ppm of cerium oxide NPs was the template for quantitative real-time PCR in the iCycler iQTM. A real-time detection system (Bio-Rad, Hercules, CA, USA) was used with SYBR_ Premix Ex Taq II (Takara Co. Ltd., Japan) for selected genes such as superoxide dismutase SOD[Cu-Zn], metallothionein (MT_2) and its isoform (we highly appreciate this reviewers precise comment) and actin 1 genes. (Karakoti et al., 2012)**.** The sequences of primers provided by NCBI (National Center for Biotechnology) (http://www.ncbi.nlm.nih.gov). The sequences **(5′—3′)** of forward (F) and reverse (R) primers. Primers were purchased from Eurofins-Genomic (Germany). Accession number and sequence of primers used are shown in Table 1:

Investigation of ultrastructure by transmission electron microscope

Leaves (0.5–4mm in length) from randomly selected plants (15 days old) were harvested after 24h from the last spraying, preserved overnight in 2.5 glutaraldehyde (v/v), and then rinsed three times with same phosphate buffer saline. The specimens were post-fixed for 1h in 1 percent OsO4, followed by three washings in 0.1M PBS (pH 7.4), each lasting 10min. Samples were rinsed in a graduated sequence of ethanol concentrations (50, 60, 70, 80, 90, 95, and 100 percent) for 15-20min at a time, followed by a 20min wash in pure acetone. After that, the samples were placed within resin and left there overnight. Ultrathin slices of control and leaves sprayed with 500ppm CeO_2 NPs were made, placed on copper grids examination by a transmission electron microscope (JEOLTEM-1010EX, Tokyo, Japan) (Karakoti et al., 2012).

TABLE 1. The sequences (5′—3′) of forward (F) and reverse (R) primers of SOD and MT genes

Gene name	Accession number	Sequences of primers (5′—3′)
SOD	AF540558	F: ACGGTGTGACCACTGTGACT R: GCACCGTGTTGTTTACCATC
MT	GU189581	F: TCTTGCTGTGGAGGAAACTG R: AGCCCAAGTCTGGGTACATC
Actin gene	FJ529167	F: TTGGGATGGACCAGAAGG R: TCAGGAGCAATACGGAGC

Statistical analysis

All experiments were repeated three times, and results were represented as means ± SEM. Statistical analysis was performed using GraphPad prism, version 5, (USA), one-way ANOVA analysis, with significant differences at P≤ 0.05.

Results

Properties of cerium oxide nanoparticles

The absorption spectrum of Ce $(NO_3)_3.6H_2O$ and CeO_2 NPs at 0, 15, 30, and 60 min. showed various peaks at 270 nm with increases elevation in absorbance at different time intervals, as shown in Fig. 1A. the structural properties of CeO_2 NPs was showed by XRD pattern. This figure shows that when the crystallinity was investigated by the XRD technique, the XRD spectrum of CeO_2 NPs showed peaks at 2θ = 28.5°, 33.0°, 47.4°, 56.2°, 59° and 69.3° corresponding to the (111), (200), (220), (311), (222) and (400) lattice planes, respectively (Fig. 1B). The peak size was detected at 19.0 nm, respectively (Fig. 1C). The zeta potential of NPs, which is defined as the characteristic impedance around all NP surfaces resulting from the attachment of the surface charge units with the opposite polarity members of the solvents of the NP solution, is typically used to indicate the longevity of NPs. In general, the greater the relative level of the zeta potential (either +ve or -ve), the stronger the attraction between the atoms that need to assemble and, as a result, the more stable the NP. The zeta potential of CeO_2 NPs was reported to be −18.8mV at pH 7.5, reflecting its low value, therefore it remained stable for long time (Fig. 1D).

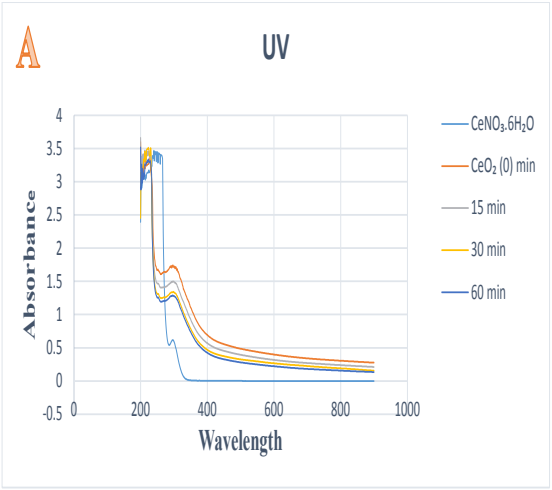

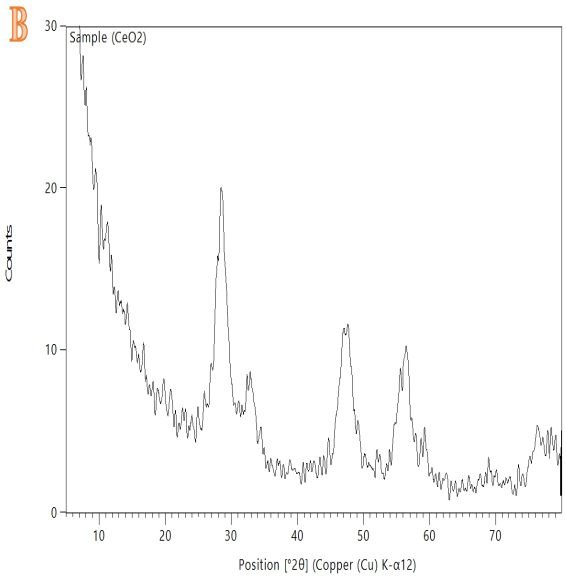

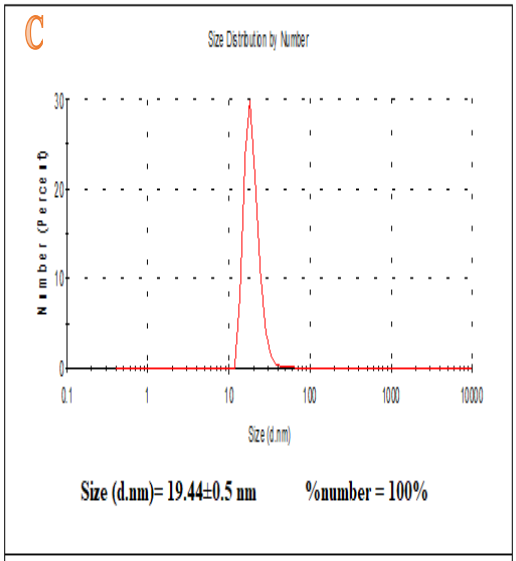

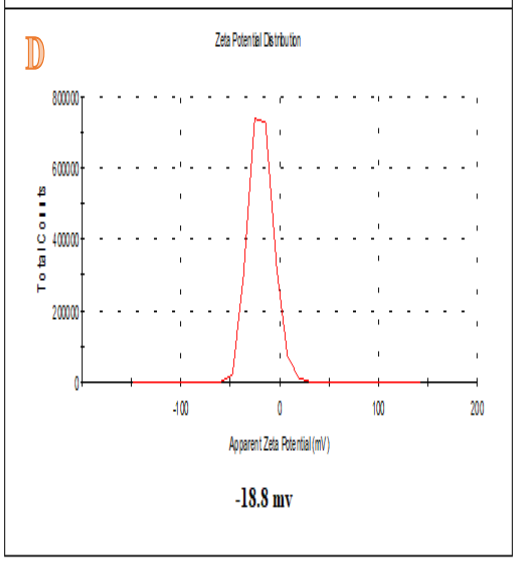

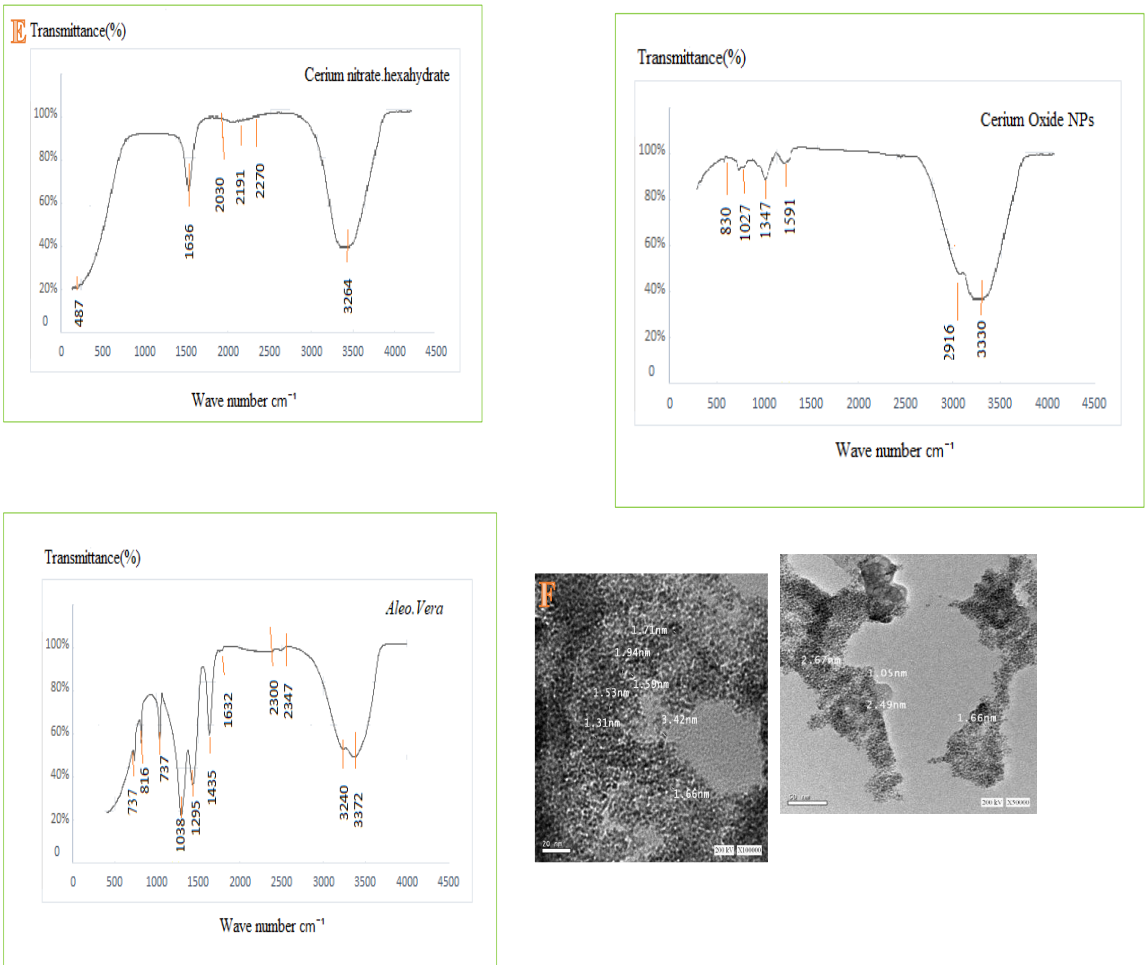

Fig. 1. Characterization of cerium dioxide nanoparticle, (A) UV–Vis absorbance of Ce $(No_3)_3.6H_2O$ and CeO_2NPs, at 15, 30 and 60min, (B) XRD pattern of CeO_2NPs, (C) Particle size of CeO_2NPs, (D) Zeta potential of CeO2NPs, (E) FTIR spectrum of Ce $(No_3)_3.6H_2O$, Aleo vera extract and CeO_2NPs respectively, (F) TEM for CeO_2NPs (5000X and 15,000X magnifications)

Analysis of FTIR spectra showed that the extract contains a phenolic −OH group and carboxyl (C-O) group. The band at 3410.23cm^{-1} in the spectrum of pure aloe vera was contributed by the OH group of carbohydrate monomers, including mannose and uronic acid; the band at 2926.03cm^{-1} indicated the presence of aliphatic CH and CH2 groups, and bands at 1610.88, 1493.83, 1244.27, 1060.69, and 876.93cm^{-1} showed -C-O stretching; asymmetrical and symmetrical –COO- stretching of carboxylate molecules. However, *Aloe vera* peaks at 3410.23, 1060.69, 876.93, 772.72 and 621.90cm^{-1} were moved to lower wave numbers, such as 3384.14, 1075.62, 848.60, 747.98, and 676.86 cm^{-1}, after CeO_2NP was formed, demonstrating participation of the C-N, -C, -H, and -OH groups in CeO_2 NP creation. Additionally, the peaks at 1610.88, 1493.83, and 1244.27cm^{-1} were eliminated, indicating that the relevant groups directly oxidized Ce ions. therefore, clearly outside the surface of CeO_2 NP as shown in Fig. 1 E. These was 3.42±1.05nm in size, practically spherical in form, and were seen along with CeO_2 NPs in the TEM image. The crystallized character of the NPs was represented in the enlarged particle image, which is displayed in Fig. 1F.

Changes in morphological parameters of Brassica napus

The results indicated that the spraying of leaves of *Brassica napus* dramatically increased (P≤ 0.05) the fresh and dry weights of plants at a concentration of 500 ppm of CeO_2 NPs as shown in Figs. 2, and 3A, B. Furthermore, the root and shoot lengths were increased upon foliar application of CeO_2 NPs with the highest impact detected at 500 ppm (P≤ 0.05), as shown in Fig. 3 C and D.

Fig. 2. Foliar application of various concentrations (A: Control, B: 250, C: 500 and D: 1000ppm) of biosynthesized CeO_2NPs. Various concentrations of biosynthesized nanoparticles were sprayed on leaves of *Brassica napus* for two weeks every 48h lead to various alterations in morphological parameters of root, and shoot lengths

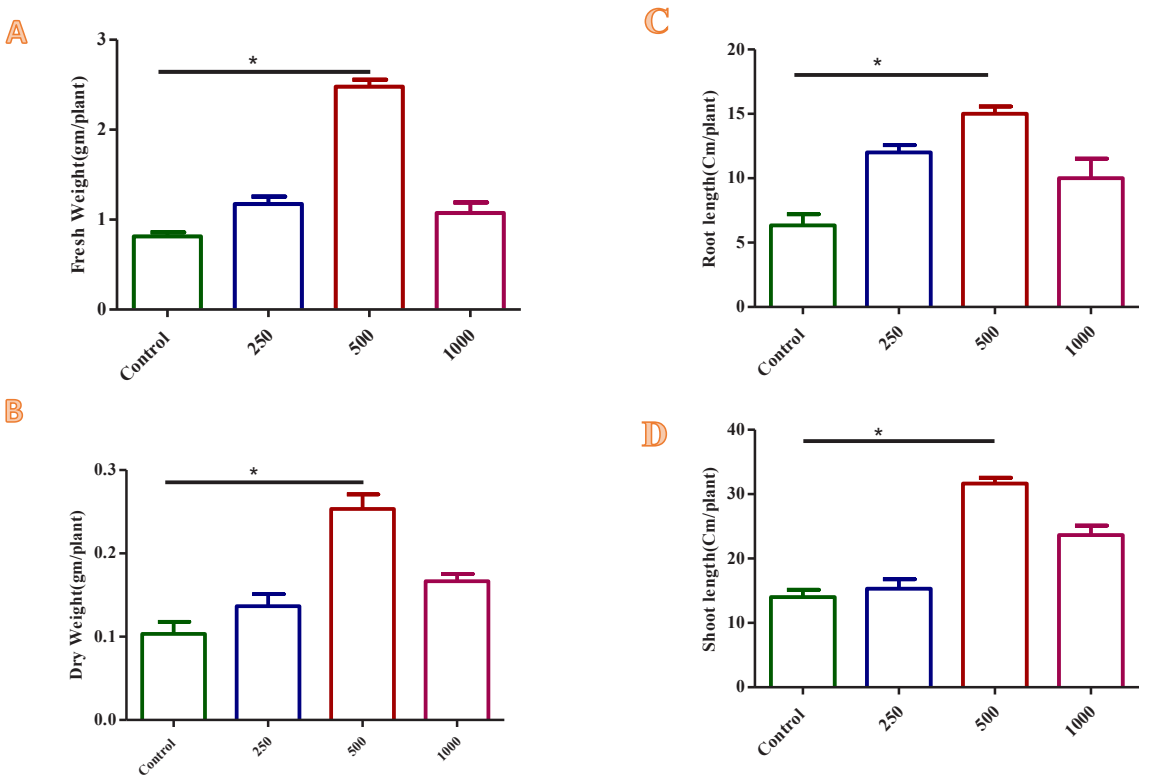

Fig. 3. Foliar application of CeO_2NPs on morphological criteria of *Brassica napus* 45 old days; Bar charts depicts comparisons of means for (A) Fresh weight (gm/ plant), (B) Dry weight g/ plant), (C) Root length (cm/ plant) and (D) Shoot length (cm/plant) for control and upon foliar application of 250, 500 and 1000ppm of CeO_2 nanoparticles, on the growth parameters of *Brassica napus* plants [Data are expressed by means± S.D, where (*) ≤ 0.05 considered as significant]

The content of cerium (Ce) in Brassica napus leaves

The results were recorded from three different samples. Ce was not detected in control samples, while spraying 250, 500 and 1000 ppm CeO_2 Nps resulted in concentration of 160 ± 4, 137 ± 6 and 130 ± 7ppm, respectively, within *B. napus* leaves as shown in Table 2.

TABLE 2. Level of Cerium concentrations (ppm) in *Brassica napus* leaves and after spraying 250, 500 and 1000ppm of CeO_2 nanoparticles [Data are expressed as means ± S.D]

Treatments	Cerium conc. in leaves mg/ kg =mg/L=ppm
C	0 ± 0
250ppm	160± 4
500ppm	137± 6
1000ppm	130±7

Impact of 500 ppm of CeO_2 NPs on ultrastructure examination of Brassica napus leaves

The ultrastructural changes in the control and treatment of 500 ppm of CeO_2 Nps on *B. napus* leaves are shown in Fig. 4. regularly structured cell walls with organized chloroplasts containing properly organized thylakoids with rounded mitochondria could been seen in control *B. napus* leaves. However, treatment with 500 ppm of CeO_2 NPs led to alteration of ultrastructure of *B. napus* leaves, including condensed thylakoid structures, enlarged mitochondria, and big spaces inside cells. Regular nuclear structures with nuclear membranes could be seen in control and treatment leaves.

Impact of various concentrations of CeO_2 NPs on histochemical staining of Brassica napus leaves

Staining of *B. napus* leaves reflected various responses of different CeO_2 Nps treatments on NBT. The production of O_2•- in *B. napus* leaves was studied by processing leaves with NBT stain, which created dark spots. Furthermore, under elevated levels of CeO_2 NPs, more dark spots of blue formazan could be seen on the leaves. Indicating, a higher accumulation of superoxide anion radical O_2•- in *B. napus* leaves, particularly at 500 ppm of CeO_2 NPs treatment as revealed by dark spot formation in the leaves (Figure 5).

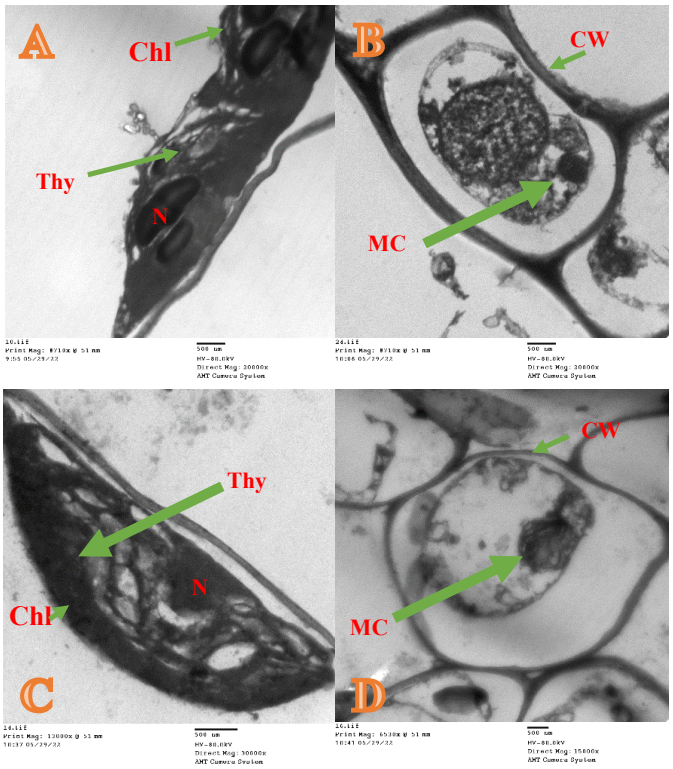

Fig. 4. Electron micrograph of *B. napus* leaf mesophyll of under (A, B) Control showing developed chloroplast (Chl), thylakoid membranes (Thy), mitochondria (MC), Nucleus (N) and regular structure cell wall (CW), while (C, D) upon spraying 500ppm of CeO_2 NPs denser structures could be seen in the sections with bigger size of mitochondria, condensed thylakoid membranes and enlarged space inside cells could be seen

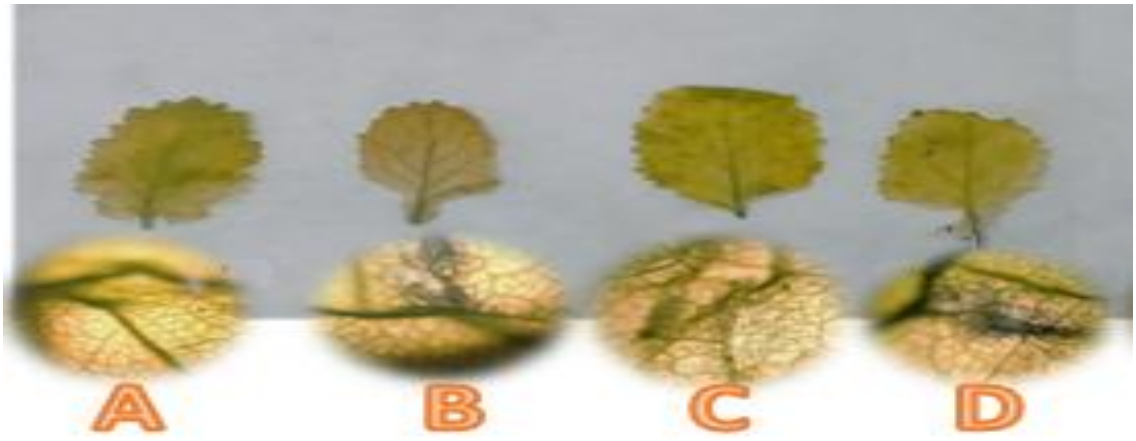

Fig . 5. Staining of *Brassica napus* leaves showing oxidative stress using nitro blue tetrazolium (NBT) upon spraying of 250, 500 and 1000ppm of CeO_2 nanoparticles where dark dots represent by oxidative stress

Impact of various concentrations of CeO_2 NPs on oxidative stress parameters

Superoxide radicals were measured in *B. napus* control plants and after foliar application with 250, 500, and 1000 ppm of CeO_2 NPs. Levels of superoxide radical decreased at 250 and 1000ppm and reached a maximum significant reduction level ($P \leq 0.001$) at 500 ppm CeO_2 NPs. Meanwhile, the level of H_2O_2 in *B. napus* leaves was dramatically increased upon spraying with 500 ppm CeO_2 NPs relative to the control. However, treatment with 250 and 1000ppm of CeO_2 NPs notably increased H_2O_2 levels in treated ,as shown in Fig. 6 A, B. MDA content was dramatically reduced after treatment with 500 ppm CeO_2 NPs, while with 250 and 1000 ppm CeO_2 NPs did not affect MDA content in *B. napus* relative to the control (Fig. 6 C).

Lipoxygenase enzyme levels did not differ under 250, 500 and 1000 ppm of CeO_2 NPs and did not significantly differ from the control (Fig. 6 D).

Impact of various concentrations of CeO_2 NPs on antioxidant enzymes

Super oxide dismutase (SOD), peroxidase (POD) and, catalase (CAT) enzymes were dramatically elevated ($P \leq 0.05$) upon spraying with 500 ppm of CeO_2 NPs compared to the control (Fig. 7). The enzymes levels were slightly increased under 250 and 1000 ppm of CeO_2 NPs relative to the control group (Fig. 7).

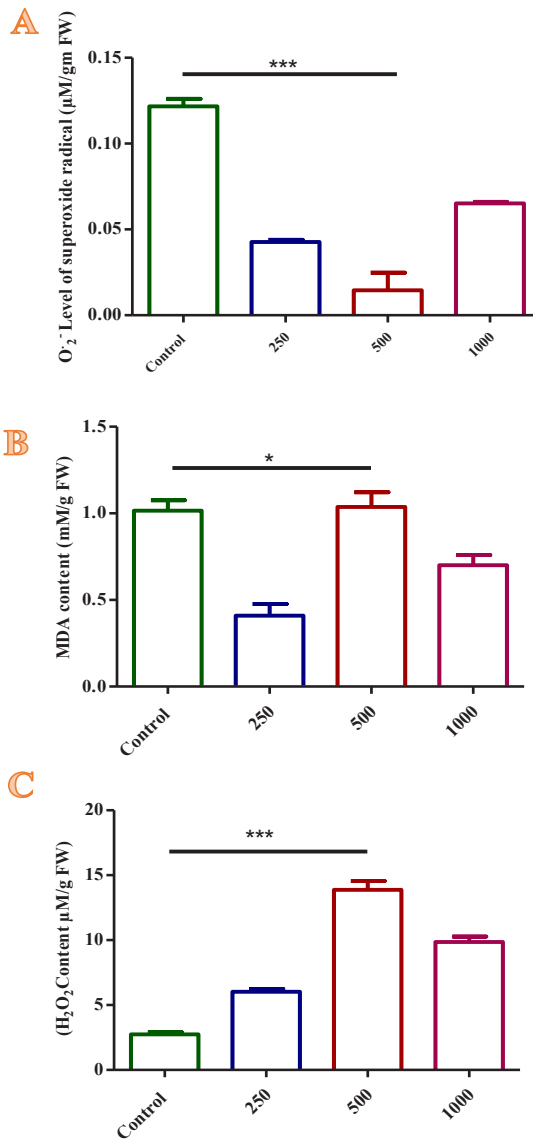

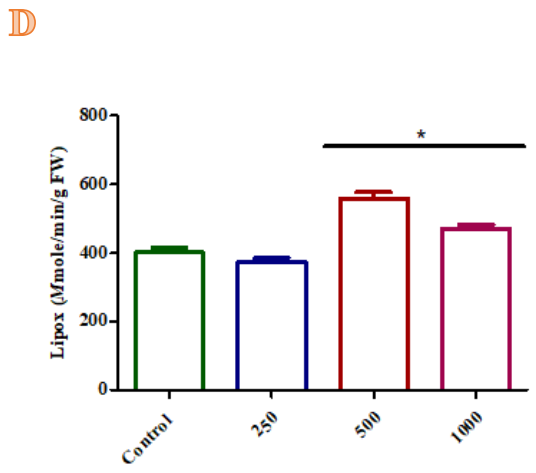

Fig. 6. Lipid peroxidation explain oxidative stress on *Brassica napus* leaves; Bar charts depicts comparisons of means (A) Level of superoxide anion radical O_2•- (µmol/g F.W), (B) H_2O_2 content (µmol/gm F.W), (C) MDA content µmol/g F.W and (D) Lipoxygenase enzyme (U/min/g F.W) [Data are expressed by means± S.D, where (*) ≤ 0.05 considered as significant)]

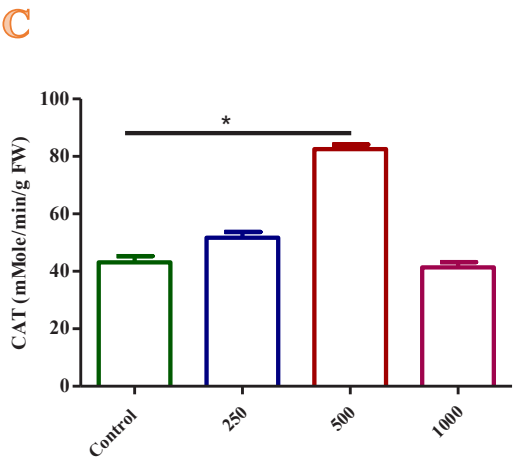

Fig. 7. Bar charts depicts comparisons of means for Antioxidant enzymes, (A) SOD (SOD activity Unit min-¹ g-¹ FW), (B) POD (POD activity µmol tetra-guaiacol formed min-¹g-¹ FW) and (C) CAT (CAT activity µmol H_2O_2 reduced min-¹g-¹ FW) for control and upon foliar application of 250, 500 and 1000ppm of CeO_2 nanoparticles, on the growth parameters of *Brassica napus* plants [Data are expressed by means± S.D, where (*) ≤ 0.05 considered as significant)]

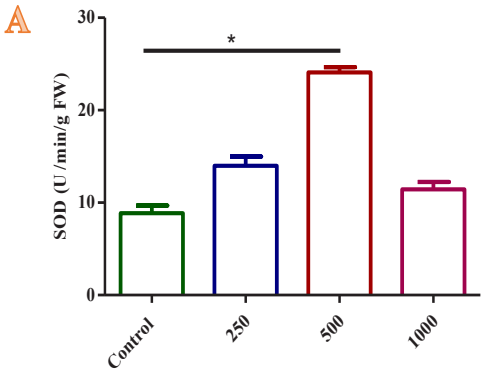

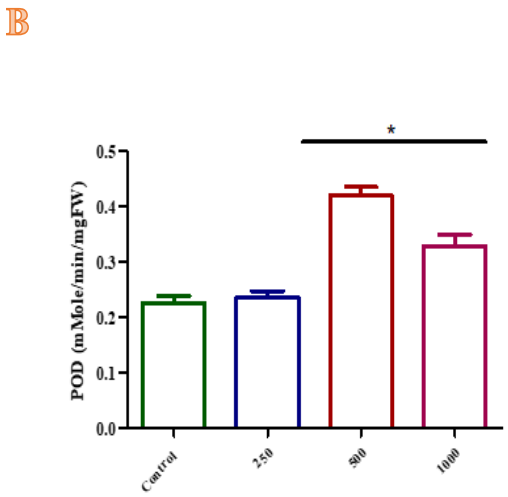

Impact of various concentrations of CeO_2 NPs on antioxidant compounds

Phenol content and ascorbic acid levels were significantly increased (P≤ 0.05) upon spraying with 500ppm of CeO_2 NPs compared to the control, while foliar application of either 250 or 1000ppm of CeO_2 NPs for *B. napus* resulted in a small elevation of phenol content and ascorbic acid levels. However, tocopherol concentration was significantly decreased (P≤ 0.05) after application of 500 ppm CeO_2 NPs compared to control group. It could be noticed that using 250ppm CeO_2 NPs did not alter tocopherol concentration, and a slight decrease in tocopherol concentration could be detected upon spraying *B. napus* with 1000 ppm of CeO_2 Nps (Fig. 8).

Impact of various concentrations of cerium dioxide nanoparticles on physiological parameters

Chlorophyll a, b contents were significantly increased after foliar application of 500 ppm of CeO_2 NPs compared to control group (P≤ 0.05). Use of 250 and 1000ppm CeO_2 NPs increased chlorophyll a level but did not affect chlorophyll b compared to control group (Fig. 9 A, B).

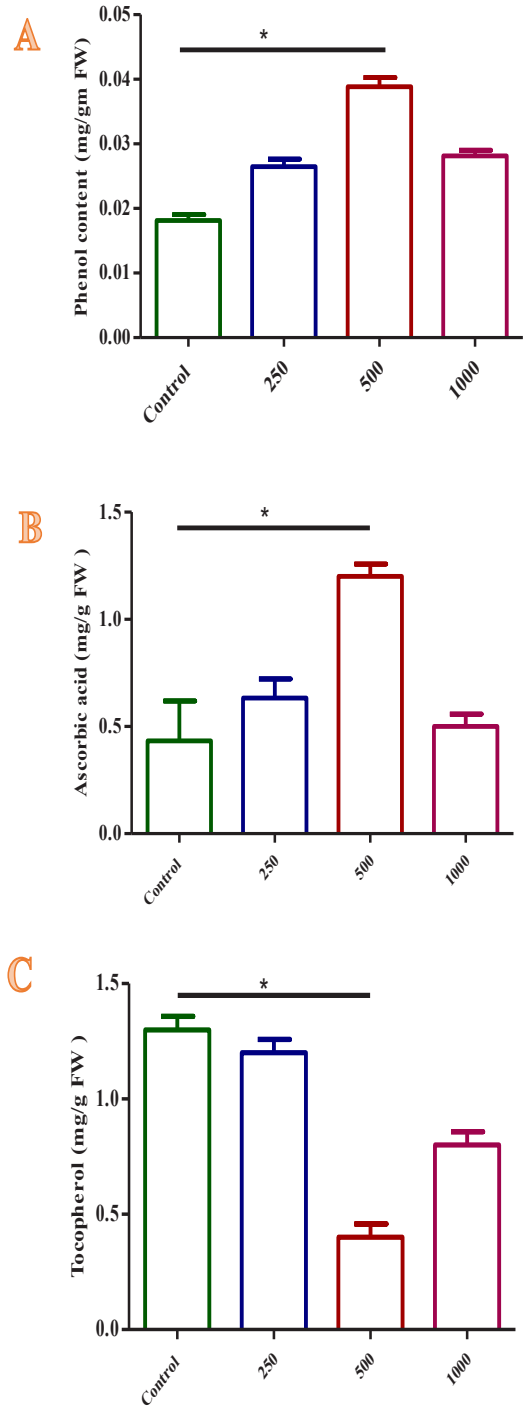

(Fig. 8) Bar charts depicts comparisons of means for Antioxidant compounds, (A) Phenol content (mg/ g F.W), (B) Ascorbic acid (mg/ g F.W) and (C) Tocopherol (mg/ g F.W) for control plants and upon foliar application of 250, 500 and 1000ppm of CeO_2 nanoparticles, on the growth parameters of *Brassica napus* plants [Data are expressed by means± S.D, where (*) ≤ 0.05 considered as significant]

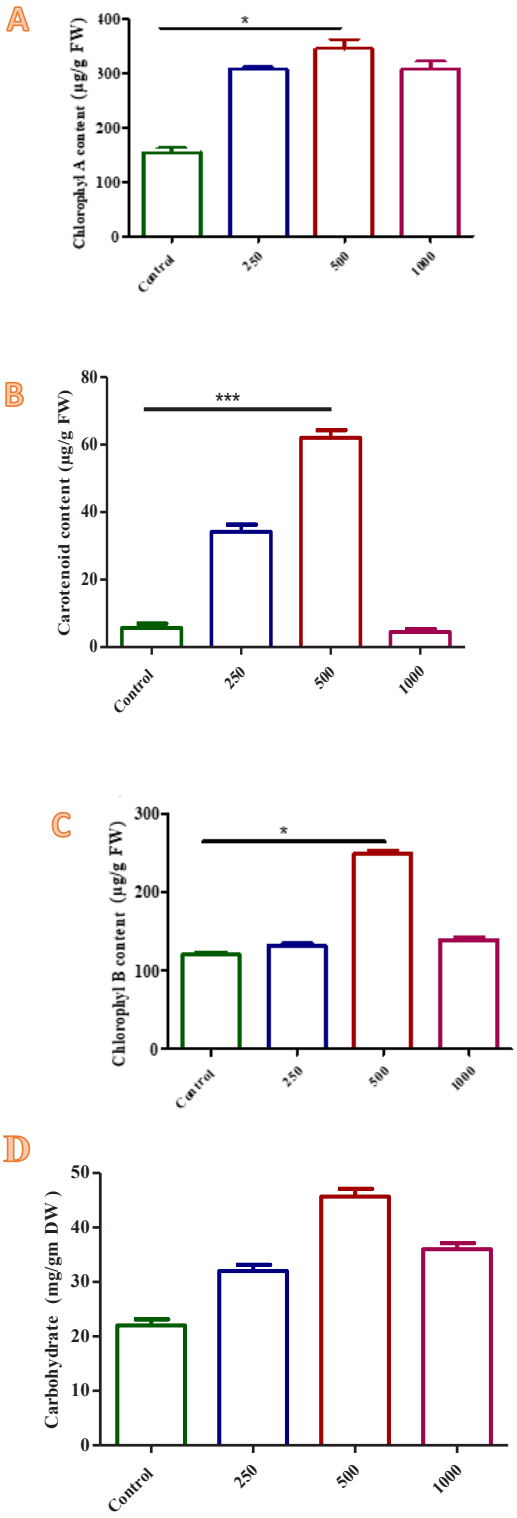

Fig. 9. Bar charts depicts comparisons of means for (A) Chlorophyll A (µg/g F.W), (B) Chlorophyll B (µg/g F.W), (C) Carotenoids (µg/ g F.W) and (D) Carbohydrates (µg/g D.W) for control and upon foliar

application of 250, 500 and 1000ppm of CeO_2 nanoparticles, on the growth parameters of Brassica napus plants [Data are expressed by means± S.D, where (*) ≤ 0.05 considered as significant, while (***) ≤ 0.001 considered as significant]

Carotenoid levels were dramatically increased (P≤ 0.001) upon spraying of 500ppm CeO_2 NPs compared to control group. Use of 250 ppm of CeO_2 NPs increased the carotenoids concentration, while application of 1000ppm of CeO_2 NPs did not increase carotenoid concentration relative to untreated plants (Fig. 9 C).

Total carbohydrate concentration was slightly increased upon spraying either 250 or 500 or 1000ppm of CeO_2 NPs compared to control group (Fig. 9 D).

Impact of various concentrations of cerium oxide nanoparticles on gene expression

Expression of SOD gene transcript levels has an essential function in stress and SOD isoforms, which in this study included cytoplasmic (Cu-Zn SOD) form. However, the MT gene is a biomarker, and its isoform (BnMT2) protects plants from metal burden and plays a role in scavenging of ROS. Expression values of SOD and MT genes were measured by real-time PCR in control leaves and under treatment with 250, 500 and 1000ppm of CeO_2 NPs**.** At concentration of 500 ppm of CeO_2 NPs there were a significant difference in both SOD and MT levels relative to control *B. napus* leaves. under treatment with 250 and 1000ppm of CeO_2 Nps there was an increase in SOD and MT levels, with a non-significant difference relative to control leaves of *B. napus* (Fig. 10 A, B).

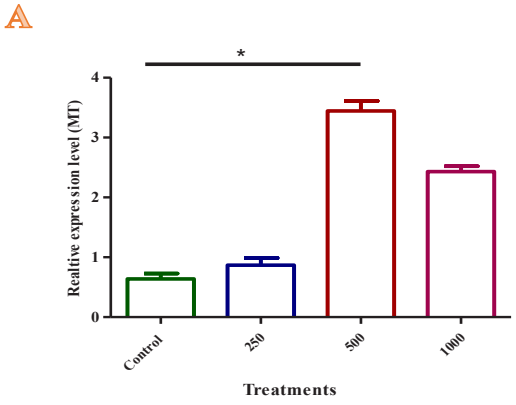

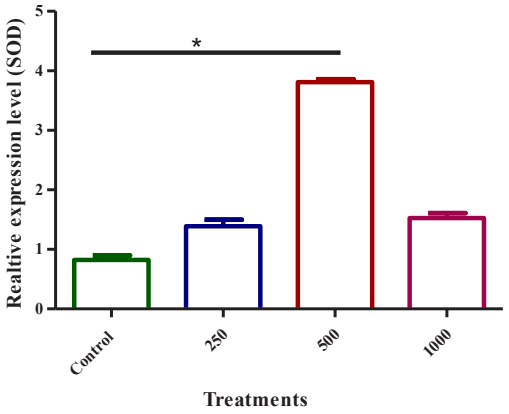

Fig. 10. (A) Levels of expression of antioxidant and stress genes including (SOD and MT) upon spraying of 250, 500 and 1000ppm of CeO_2 nanoparticles on *Brassica napus* leaves [Data are expressed by means± S.D, where (*) ≤ 0.05 considered as significant)]

Discussion

Changes in temperature produce different-sized nanoparticles with different properties, and this could be responsible for the particles strong antioxidant capacity (Kar et al., 2009; Mao et al., 2021). CeO_2 NPs are known for their dual oxidation state, Ce^{+3} to Ce^{+4}, which improves their catalytic activity in biosystems (Huang et al., 2017). Zeta potential is regularly used to distinguish the colloidal stability of macromolecules and particles suspended in liquid (Ramaye et al., 2021). Zeta potential stability, which is defined as the potential difference around the NP surface resulting from the association of the surface charge groups with the opposite charge groups of the solvent of the NP suspension. The present study was showed more nanoparticle stability (Fig. 1D) with a zeta potential –18.8mv at pH 7. Changes in temperature produce different-sized NPs with different properties, and this could be responsible for the particles' strong antioxidant capacity (Kar et al., 2009; Karakoti et al., 2012). In the present study, elevation of temperature to 60°C led to the production of almost spherical and well-dispersed of CeO_2 NPs with a size ranging from 1.05 to 2.67nm. TEM showed the morphology and size distribution from the enlarged image of a particle, presented in the inset of Fig. 1F and applied in this study. Nevertheless, methods of synthesis at room temperature were informed to produce nanoceria with beneficial

antioxidative properties, whereas methods at high temperature produce NPs with deleterious pro-oxidative properties; moreover, as opposed to high-temperature, ambient temperatures synthesis creates smaller NPs with a uniform size and higher ratio of Ce^{3+}/Ce^{4+} concentrations as well as a high antioxidant capacity due to the particles were affinity for alteration in enhanced environment oxidation state (Karakoti et al., 2012). Additionally, methods of synthesis of CeO_2 NPs at high temperatures were reported to produce generally crystalline CeO_2 -NP of larger size (>25nm), whereas methods at room temperature, produce much smaller and nearly spherical particles with loss of crystallinity were formed. The lattice fringes the d-spacing values, were about 3.1Å, 3.15Å, and 3.16Å, i.e., very near to the lattice spacing of 111 plane (3.124Å) of CeO_2 NPs (Tiseanu et al.,2011). When the crystallinity was examined by the XRD technique, the XRD spectrum of CeO_2 NPs described peaks at 28.20, 47.40, and 56.20. the lattice planes of CeO_2 NPs crystals matching the angles were (111), (220) and (311) respectively, and were same after one year with the same angle and lattice planes. The lattice parameters from powdered XRD data were found to be a = b =c = 5.419 Å, α= β= γ =90° using Panlytical X'pert Pro software. The acquired lattice parameters for nanoceria were also detected. The XRD pattern of CeO_2 NPs powder indicates broad peaks, which confirmed the formation of small-sized nanoparticles. The particle size of the nanoparticles was determined using the Scherrer's relation d= (0.9 l)/ (b cos q) where, l is the wavelength of X-rays used, q is Bragg's angle [20], and b is the full width at half maximum in radians. For the different reflection peaks of the XRD pattern, the particle size was estimated and the average size of nanoparticles of the sample was found to be around 2nm according to Blanton & Majumdar (2013). Such characteristic crystal planes in CeO_2 NPs have also been reported (Tiseanu et al., 2011). Analysis of FTIR spectra showed that the extract contains a phenolic −OH group and carboxyl (C-O) group. The band at 3410.23 cm^{-1} in the spectrum of pure aloe vera was contributed by the OH group of carbohydrate monomers, including mannose and uronic acid; the band at 2926.03cm^{-1} indicated the presence of aliphatic CH and CH2 groups; bands at 1610.88, 1493.83, 1244.27, 1060.69, and 876.93cm^{-1} were from -C- O stretching; asymmetrical and symmetrical –COO- stretching of carboxylate molecules. However, *Aloe vera* extract peak at 3410.23, 1060.69, 876.93, 772.72 and 621.90cm^{-1} were moved to lower wave numbers, such as 3384.14, 1075.62, 848.60, 747.98, and 676.86 cm^{-1}, after CeO_2 NPs was formed, demonstrating participation of C-N, -C, -H, and -OH groups in CeO_2NP creation. Additionally, the peaks at 1610.88, 1493.83, and 1244.27cm^{-1} were eliminated, indicating that the relevant groups directly oxidized Ce ions. in the same line, (Giri, 2018) The FTIR pattern of CeO_2 NPs is shown that the broad absorption band positioned around 3400cm^{-1} resembles the O–H stretching vibration of the remaining water and hydroxyl groups, although the absorption band at 1630cm^{-1} was due to the crosscut bending manner of water. The complex bands detected at around 1518, 1350, and 1053cm^{-1} were due to undesirable residues in the sample. The band at 848cm^{-1} matched the metal–oxygen bond. The assignments of CeO_2 NPs for the absorption peak or bands for CeO_2 NPs are provided. It is known that cerium can exist either in Ce (III) or in Ce (IV) oxidation states; however, Ce(IV) is yellow to red in color and Ce(III) is normally colorless (Singh et al., 2011). At the same time, cerium in dual oxidation states absorbs UV light with two distinctive absorption peaks at Ce(III) state in the (230–260) nm range and the Ce(IV) state in the (300–400) nm range (Emsley, 2011). Absorption in the near ultraviolet region arises from electronic transitions within the sample. Consequently, our method explains that nanoceria at time different time intervals spectrum appeared around 270-360nm. While, in the UV region, the spectrum showed a strong absorption band in line for the charge transferred transitions between the states of energy, no absorption was detected in the wavelength range of 500-900nm. The self-assembly of the nanoparticles in UV region was shown due to The breadth of the absorption shoulder. In addition, CeO_2 NPs are very effective at UV filtration. CeO_2 has a UV limit threshold at about 370 nm. Goharshadi et al. (2011) confirmed that a maximum of UV light (200-350nm) may be blocked by CeO_2 NPs, which makes CeO_2 NPs an extremely promising material for UV blocking in coating materials on sunglasses, parasols, and sunscreens. In this way, the concentrations of NPs commonly follow the order of root > shoot > fruit > grains in plant tissue subsequently root exposure (Pullagurala et al., 2018). According to the Food and Drug Authority (FDA), the antioxidant power of cerium and its highly biocompatible mineral is due to the charges on its surface. Therefore, as

unique of the rare earth elements (REE), in agricultural practices, Ce has been broadly used as a preservative in fertilizers to increase the yield of crops (Yuan et al., 2001). Even though valuable effects of cerium on plant biology be able to be recognized to a significant stimulation of photosynthetic activity, chlorophyll biosynthesis, and antioxidative capacity too (Hong et al., 2014). Several studies suggested that the phytotoxic effects of CeO_2 NPs on plants, containing the physiology and molecular responses of plants to CeO_2 NPs, were mostly caused by the oxidative stress sustained by CeO_2 NPs and can be explained from the biochemical features (Ma et al., 2015). Plants growth inhibition due to the loss of cellular turgor or to a decrease extensibility of the cell wall (d'Aquino et al., 2009). Inhibitory effects be able to also due to a reducing efficiency of certain enzymes included in energy utilization and plant metabolism, reduce cell division (Mali & Aery, 2009). The reported results allow us to discuss some important aspects of the protective action against the stress might cause by cerium oxide nanoparticles. So, many researchers have reported that using CeO_2 NPs at the right concentrations accelerates photosynthesis and increases plant development by increasing the photosynthetic rate (Kar et al., 2009; Salehi et al., 2021). In the present study concentrations 250, 500 and 1000 ppm of CeO_2 NPs were sprayed on leaves of *B. napus* enhancing morphological parameters including root length, shoot length, fresh weight, and dry weight especially at 500ppm ($P \leq 0.05$). Furthermore, the large surface area and compact size of NPs make it easier for them to enter cells, which helps to boost growth of plants. Given the beneficial effects of CeO_2 NPs on crop fresh, and dry weight and length, it would appear that their results confirmed a number of growth-related variables enhances crop yield. (Singh & Husen, 2019; Khan et al., 2021). Ma et al. (2010), reported that exposure to a 1000mg L^{-1} CeO_2-NPs suspension for 5 days had no adverse effect on the seed germination and root elongation of cabbage, tomato, radish, rape, wheat, and cucumber. The plants had significantly more biomass with compared to control which treated with 500mg $nCeO_2$/L, and determines positive physiological response. Suchlike positive response has also been described in soybean, wherever the root growth was improved upon nanopowder of CeO_2 exposure (Lopez-Moreno et al., 2010). our study was in disagreement in that only the leaves of plants treated with 500mg $nCeO_2$/L after seven day of exposure (DE), displayed significant increase in biomass with compare to control and other treatments. However, there were no significant effects on biomass production. after 15 DE. No noticeable effects on biomass upon exposure to CeO_2 NPs for more than 8 days reported in tomato, and cucumber. (López-Moreno et al., 2010), and soybean (Priester et al., 2012). Ce was detected in *b. napus* leaves, and the accumulation of Ce increased with dose concentration, so our result disagrees with pervious observations that Ce reduces the germination of tomato (*Solanum lycopersicum*) and radish (*Raphanus sativus*) seeds, which is related to the higher availability and mobility of the elements in the soil (Thomas et al., 2014). Furthermore, Ce application to the soil can increase the activity of the photosystem II (PSII) and stimulate N assimilation, thereby stimulating plant development (Zhao et al., 2012). The production rates of ROS were directly to the metabolic pathways, such as mitochondrial photosynthesis or respiration. Contrariwise, they similarly feed NADPH-producing metabolism such as the oxidative pentose-phosphate pathway was elaborated in the antioxidative processes (Couée et al., 2006). Plants have both enzymatic and non-enzymatic defensive mechanisms. SOD and CAT enzymes are a components of the original enzymatic defense mechanism. SOD controls the removal of superoxide radicals and serves as the first line of defense against free radicals (Kumar et al., 2017). The accumulation of excess H_2O_2 is prohibited by POD, APX and CAT. As effect of SOD reaction H_2O_2 increased was complemented by enhanced enzymes activities to decay it. Therefore, under stress conditions, CAT and APX coordinate with SOD and play a significant role in H_2O_2 scavenge (Farooq et al., 2016). Plants ability to overcome oxidative stress mainly depends on SOD activity induction and consequently on the up-regulation of other downstream antioxidant enzymes. The present results show that application of 500ppm CeO_2 NPs significantly enhanced ($P \leq 0.05$) CAT and SOD levels and increased POD levels in *B. napus* so the level of phenolic compounds increased. Phenols are organic compounds which contain a hydroxyl group attached to aromatic ring which, exist in leafy vegetables are essential for scavenging free radicals and reducing the burden of oxidative illness (Côté et al., 2010; Oberoi & Sandhu, 2015). Rapeseed plant meal contain a high content of phenolic acid esters,

mostly sinapate esters, that cause a bitter taste and dark color in rapeseed meal also derived protein products. In rapeseed, Sinapic acid is the greatest common phenolic acid, also a powerful scavenger of free radicals (Lotfi et al., 2010). In accordance with our present study application of 500ppm CeO_2 NPs significantly enhanced (P≤0.05) phenol content and ascorbic acid. α-tocopherol can be transferred liberally within the lipid membrane, due to its fluidity so providing membrane protection (Racchi et al., 2013). The content of tocopherol which plays a protective role in *B. napus* was significantly decreased (P≤0.05) at 500ppm CeO_2 NPs. However, the stimulation of biosynthetic enzyme activities might be attributed to increase of chlorophyll content to stress tolerance by triggering chlorophyll biosynthesis-related gene expression levels under stress conditions (Wu et al., 2014). Cerium dioxide nanoparticles play a role in chlorophyll biosynthesis and the chloroplast defense integrity against damage brought on it by salinity According to a study on sweet pepper, adding (0.2mM) of CeO_2 NPs to the soil under conditions of 60mM salt content enhanced number of leaves, photosynthesis, total chlorophyll, plant dry weight, and SOD activity. This, in turn, activated the antioxidant protection system, improved ion uptake, concurrently decreased ethylene yield within the plants, enhanced photosynthetic rate, and helped the plants stay alive in harsh circumstances (Essbihi et al., 2021). In the present study it could be noticed that application of 500 ppm of CeO_2 NPs led to significant elevation of chlorophyll a, Chlorophyll b (P≤ 0.05) and dramatic increased of carotenoids (P≤ 0.001) but did not affect carbohydrates levels in all the concentrations applied. The amount of chlorophylls and carotenoids in the plants can be thought as a biological indicator of their resistance to stress; changes in these amount show how the plant reacts to stress (Zaman et al., 2019; Maoka, 2020). It was appeared that CeO_2 NPs were highly absorbed upon spraying on leaves which is in agreement with (Hayder et al., 2020) who reported the effective transfer of cerium and cupper nanoparticles to the aerial parts of the radish plant. Moreover, the present study revealed the role of 500ppm of CeO_2 NPs in downregulation of the lipid peroxidation process. The main plant biomarkers of oxidative damage, H_2O_2 and O_2 •–, were measured in the leaves and roots of B. napus under different concentration of cerium oxide NPs. The process of lipid peroxidation is an essential step in oxidative stress by generating the hydrogen peroxide (H_2O_2) though the elevation of (O_2•-), fatty acids which transformed into hazardous lipid peroxides that harm cellular membranes, enzymes, and polynucleotides (Sun et al., 2011; Hossain et al., 2012). In accordance with (Gill et al., 2015) who demonstrate how plant cells' function to maintain a balance between the active oxygen free radical's generation and removal. The antioxidant system enhanced therefore displays greater plasma membrane integrity result in lower lipid peroxidation when under stress. (Safi et al., 2020). Though, CeO_2-NPs led to oxidative stress and caused lipid peroxidation at a higher dose (500mg/L), also, increased electrolyte leakage (Rico et al., 2013). In barely plant under drought stress has been represented that LOX activity increased also enhance the transcription of LOX-related genes, so amount of this enzyme raises (Kubis, 2006). In a negative correlation with our result, LOX enzyme were not affected in all treatment compared to control.

Expression levels of stress related genes were assessed by molecular evaluated RNAs isolated leaves of *B. napus* sprayed with various concentrations of CeO_2 NPS cultivated plants. Previous studies showed that Cd and As stress promoted metalloproteins expression besides accumulation in plants (Goupil et al., 2009) These findings show that induction of As-stress tolerance in B. napus plants as it has recently shown in arsenic, copper and boron stresses so metallothionein binding protein transcript accumulation (Tombuloglu et al., 2012). Panda & Matsumoto (2010) also suggested that under aluminum stress a higher expression level of SOD, APX, CAT and GR in tolerant cultivar. While, under different metals stress like cadmium (Luo et al., 2011) and aluminum gene expression phenomena were studied also (Panda & Matsumoto, 2010). Some of the patterns for NP-mediated toxicity contain oxidative stress, genetic damage, the inhibition of cell division, cell death and inflammation (Johnston et al., 2010). In accordance with our findings, exposure of *B. napus* plants to 500ppm of CeO_2 NPS lead to dramatic up regulation of MT and SOD. In accordance with Ahn et al. (2012) reported that three MT genes were regulated under different metal burden in *Brassica rapa*.

In plants, nanoparticle-induced ROS

generation has been described that primes to membrane damage and eventually cell death (Shen et al., 2010). TEM examination in current report revealed that 500ppm of CeO_2 NPs alter the cellular organelles of *B. napus* leaves adversely. In accordance with the previous study by Ali et al. (2014), Who reported that high concentrations of heavy metals can damage the cell organelles in the leaves and roots of plants. In this respect, NPs-induced ROS generation primes to membrane damage and eventually cell death in plants (Shen et al., 2010). However, studies relating ROS generation and NP stress have been described, the afterward effects of the generated ROS on proteins and DNA are less recognized (Zhao et al., 2012). Moreover, NPs uptake and translocation through the cuticle under foliar exposure, which attends as the first guard barrier. Also, the cuticle its waxy nature prevents water loss and solute exchange. (Pollard et al., 2008).

Conclusions

The present work studied the foliar application of different concentrations of CeO_2 NPs affecting the morphological, physiological and molecular responses of *B. napus* mainly at 250,500,1000ppm and the concentration of 500 ppm showed an improvement in the morphological variables. However, the enhancement of oxidative stress due to high levels of CeO_2 NPs concentration, especially at 1000ppm led to a decrease in plasma membrane integrity. So the level of antioxidant enzyme increased to relieve the oxidative effect which confirmed at the molecular level by high stimulation of SOD gene. However, the MT gene indicates a high level of stress on the plant as a result of the high level of metals. Therefore, with regard to safe use in the agricultural sector, a protection compound must be added with nanoparticles to fully benefit from it in the hope of achieving sustainable agricultural applications.

Competing interests The authors report no conflicts of interest regarding this work.

Authors' contributions: Salma M. Awad performed the experiments, prepare and synthesis of nanoparticle, wrote the initial draft of the manuscript, perform data analysis and wrote the manuscript. Tahani A. Hathout, Samia M. El khallal, who proposed the research idea, supervised the practical work and refined the manuscript. Khaled Y. Farroh is responsible on the part of the preparation, and characterization of nanoparticles in the research.

Ethics approval and consent to participate: Not applicable

References

Aebi, H., Lester, P. (1984) Catalase in vitro. *Methods in Enzymology,* **105**, 121–126.

Ahn, O., Kim, S.H., Lee, J., Kim, H.R., Lee, H.S., Kwak, S.S. (2012) Three *Brassica rapa* metallothione in genes are differentially regulated under various stress conditions. *Molecular Biology Reports,* **39**, 2059–2067.

Ali, B., Qian, P., Jin, R., Ali, S., Khan, M., Aziz, R., Tian, T., Zhou, W.J. (2014) Physiological and ultra-structural changes in *Brassica napus* seedlings induced by cadmium stress. *Biologia Plantarum,* **58**, 131–138.

APHA (American Public Health Association) (2017) AWWA (American Water Works Association), and WEF (Water Environment Federation). "*Standard Methods for the Examination of Water and Waste Water*", 23rd edn., (Rice, E., Baird, R.B., Eaton, A, D., Clesceri, l. S. Eds.) Washington DC.

Axelrod, B., Cheesbrough, T.M., Laakso, S. (1981) [53] Lipoxygenase from soybeans: EC 1.13. 11.12 Linoleate: oxygen oxidoreductase. In: "*Methods in Enzymology*". Elsevier, pp. 441–451.

Backer, H., Frank, O., de Angells, B., Feingold, S. (1980) Plasma tocopherol in man at various times after ingesting free or ocetylaned tocopherol. *Nutrition Reports International,* **21**, 531–536

Bao, D., Oh, Z.G., Chen, Z. (2016) Characterization of silver nanoparticles internalized by arabidopsis plants using single particle ICP-MS analysis. *Frontiers in Plant Science,* **7**, 1–8.

Blanton, T.N., Majumdar, D. (2013) Characterization of X-ray irradiated graphene oxide coatings using X-ray differaction, X-ray photoelectron spectroscopy, and atomic force microscopy. *Powder Diffraction*, **28**(2), 68-71.

Cassee, F.R., Van Balen, E.C., Singh, C., Green, D., Muijser, H., Weinstein, J., et al. (2011) Exposure, health and ecological effects review of engineered

nanoscale cerium and cerium oxide associated with its use as a fuel additive. *Critical Reviews in Toxicology,* **41**, 213–229.

Couée, I., Sulmon, C., Gouesbet, G., El Amrani, A. (2006) Involvement of soluble sugars in reactive oxygen species balance and responses to oxidative stress in plants. *Journal Experimental of Botany.* **57**, 449–459.

Côté, J., Caillet, S., Doyon, G., Sylvain, L., Lacroix, M. (2010) Bioactive compounds in cranberries and their biological properties. *Critical Reviews in Food Science and Nutrition,* **50**, 666–679.

d'Aquino, L., de Pinto, M.C., Nardi, L., Morgana, M., Tommasi, F. (2009). Effect of some light Rare Earth Elements on seed germination, seedling growth and antioxidant metabolism in *Triticum durum*. *Chemosphere*; **75**, 900–905.

Doke, N. (1983) Involvement of superoxide anion generation in the hypersensitive response of potato tuber tissues to infection with an incompatible race of Phytophthora infestans and to the hyphal wall components. *Physiological Plant Pathology,* **23**, 345–357.

Dubois, M., Gilles, K.A., Hamilton, J.K., Rebers, P.T., Smith, F. (1956) Colorimetric method for determination of sugars and related substances. *Analytical Chemistry*. *ACS Publications*, **28**(3), 350–356.

Dutta, D., Mukherjee, R., Patra, M., Banik, M., Dasgupta, R., Mukherjee, M., Basu, T. (2016) Green synthesized cerium oxide nanoparticle: A prospective drug against oxidative harm. *Colloids and Surfaces B: Biointerfaces,* **147**, 45-53.

Ejaz, M., Raja, N.I., Mashwani, Z.U., Ahmad, M.S., Hussain, M., Iqbal, M. (2018) Effect of silver nanoparticles and silver nitrate on growth of rice under biotic stress. *IET Nanobiotechnology,* **12**, 927–932.

Eldarier, S.M., Abou-Zeid, H.M., Marzouk, R.I., Abo Hatab, A.S. (2020) Biosynthesis of silver nanoparticles via *Haplophyllum tuberculatum* (Forssk.) A. Juss.(Rutaceae) and its use as bioherbicide. *Egyptian Journal of Botany,* **60**(1), 25-40.

Emsley, J. (2011) "*Cerium, in: Nature's Building Blocks: An A–Z Guide to the Elements*", Oxford University Press, Oxford, pp. 120–125.

Essbihi, F.Z., Hazzoumi, Z., Aasfar, A., Amrani Joutei, K. (2021) Improving salinity tolerance in *Salvia officinalis* L. by foliar application of salicylic acid. *Chemical and Biological Technologies in Agriculture,* **8**. doi: 10.1186/s40538-021-00221-y.

Faizan, M., Bhat, J.A., Chen, C., Aleymeni, M.N., Wijaya, L., Ahmad, P., Yu, F. (2021) Zinc oxide nanoparticles (ZnO-NPs) induce salt tolerance by improving the antioxidant system and photosynthetic machinery in tomato. *Plant Physiology and Biochemistry,* **161**, 122–130.

Farooq, M.A., Gill, R.A., Ali, B., Wang, J. (2016) response to arsenic in Brassica napus L Subcellular distribution, modulation of antioxidant and stress-related genes response to arsenic in *Brassica napus L . Ecotoxicology*, *March*. https://doi.org/10.1007/s10646-015-1594-6.

Farooq, M.A., Islam, F., Ayyaz, A., Chen, W., Noor, Y., Hu, W., Hannan, F., Zhou, W. (2022) Mitigation effects of exogenous melatonin-selenium nanoparticles on arsenic-induced stress in *Brassica napus*. *Environmental Pollution,* **1**;292(Pt B):118473. doi: 10.1016/j.envpol.2021.118473.

Fortunato, A.S., Lidon, F.C., Batista-Santos, P., Leitão, A.E., Pais, I.P., Ribeiro, A.I., Ramalho, J.C. (2010) Biochemical and molecular characterization of the antioxidative system of Coffea sp. under cold conditions in genotypes with contrasting tolerance. *Journal of Plant Physiology,* **167**(5), 333–342.

Friedt, W., Snowdon, R. (2009) Oilseed rape.In: "*Handbook of Plant Breeding*", Vol. 4: Oil Crops Breeding, J. Vollmann and R. Istvan (Eds.), New York, NY: Springer, pp. 91–126.

Giri, T.K., Dey, B., Maity, S. (2018) Preparation and characterization of nanoemulsome entrapped in enteric coated hydrogel beads for the controlled delivery of capsaicin to the colon. *Current Drug Therapy,* **13**(1), 98–105.

Gill, R.A., Ali, B., Islam, F., Farooq, M.A., Gill, M.B., Mwamba, T.M., Zhou, W.J. (2015) Physiological and molecular analyses of black and yellow seeded Brassica napus regulated by 5-aminolivulinic acid under chromium stress. *Plant Physiology and Biochemistry,* **94**, 130–143.

Goharshadi, E.K., Samiee, S., Nancarrow, P. (2011) Fabrication of cerium oxide nanoparticles: characterization and optical properties. *Journal of Colloid and Interface Science,* **356**(2), 473-480.

Goupil, P., Souguira, D., Ferjani, E., Faurec, O., Hitmid, A., Ledoigta, G. (2009) Expression of stress-related genes in tomato plants exposed to arsenic and chromium in nutrient solution. *Journal of Plant Physiol*ogy, **166**, 1446–1452.

Hafez, R., Fouad, A. (2020) Mitigation of genotoxic and cytotoxic effects of silver nanoparticles on onion root tips using some antioxidant scavengers. *Egyptian Journal of Botany,* **60**(1), 133-145.

Hayder, M., Wojcieszek, J., Asztemborska, M., Zhou, Y., Ruzik, L. (2020) Analysis of cerium oxide and copper oxide nanoparticles bioaccessibility from radish using SP-ICP-MS. *Journal of the Science of Food and Agriculture*, **100**(13), 4950-4958.

Hossain, M.A., Piyatida, P., Jaime, A., DaSilva, T., Fujita, M. (2012) Molecular mechanism of heavy metal toxicity and tolerance in plants: central role of glutathione in detoxification of reactive oxygen species and methylglyoxal and in heavy metal chelation. *Journal of Botany,* doi:10.1155/2012/872875.

Hong, J., Peralta-Videa, J.R., Rico, C., Sahi, S., Viveros, M.N., Bartonjo, J., Zhao, L., Gardea-Torresdey, J.L. (2014) Evidence of translocation and physiological impacts of foliar applied CeO_2 nanoparticles on cucumber *(Cucumis sativus) plants. Environmental Science and Technology,* **48**, 4376–4385.

Huang, Y.-W., Cambre, M., Lee, H.-J. (2017) The toxicity of nanoparticles depends on multiple molecular and physicochemical mechanisms. *International Journal of Molecular Science,* **18**, 2702.

Jabs, T., Dietrich, R.A., Dangl, J.L. (1996) Initiation of runaway cell death in an *Arabidopsis* mutant by extracellular superoxide. *Science,* **273**, 1853–1856.

Jagota, S.K., Dani, H.M. (1982) A new colorimetric technique for the estimation of vitamin C using Folin phenol reagent. *Analytical Biochemistry,* **127**(1), 178–182.

Jakhar, S., Mukherjee, D. (2014) Chloroplast pigments, proteins, lipid peroxidation and activities of antioxidative enzymes during maturation and senescence of leaves and reproductive organs of *Cajanus cajan* L. *Physiology and Molecular Biology of Plants*, **20**(2), 171-80.

Javanmardi, J., Stushnoff, C., Locke, E., Vivanco, J.M. (2003) Antioxidant activity and total phenolic content of Iranian Ocimum accessions, *Food Chemistry*, **83**(4) 547-550.

Johnston H.J., Hutchison, G., Christensen, F.M, Peters, S., Hankin, S., Stone, V. (2010) A review of the in vivo and in vitro toxicity of silver and gold particulates: particle attributes and biological mechanisms responsible for the observed toxicity. *Critical Reviews in Toxicology,* **40**(4), 328–346.

Karakoti, A.S., Munusamy, P., Hostetler, K., Kodali, V., Kuchibhatla, S., Orr, G., Pounds, J.G., Teeguarden, J.G., Thrall, B.D., Baer, D.R. (2012) Preparation and characterization challenges to understanding environmental and biological impacts of ceria nanoparticles. *Surface and Interface Analysis,* **44**, 882–889.

Kar, S., Patel, C., Santra, S. (2009) Direct room temperature synthesis of valence state engineered ultra-small ceria nanoparticles: investigation on the role of ethylenediamine as a capping agent. *Journal of Physical Chemistry,* **113**, 4862–4867.

Khan, M.N., Li, Y, Khan, Z., Chen, L., Liu, J., Hu, J., Wu, H., Li, Z. (2021) Nanoceria seed priming enhanced salt tolerance in rapeseed through modulating ROS homeostasis and α-amylase activities. *Journal of Nanobiotechnology,* **19**(1), 276. doi: 10.1186/s12951-021-01026-9.

Kubis, J. (2006) Exogenous spermidine alters in different way membrane permeability and lipid peroxidation in water stressed barley leaves. *Acta Physiology Plant,* **28**, 27–33.

Kumar, D., Al Hassan, M., Naranjo, M.A., Agrawal, V., Boscaiu, M., Vicente, O. (2017) Effects of salinity and drought on growth, ionic relations, compatible solutes and activation of antioxidant systems in oleander (*Nerium oleander* L.). *PLoS ONE,* **12** doi: 10.1371/journal.pone.0185017.

Lee, J., Jeong, J.S., Kim, S.Y., Lee, S.J., Shin, Y.J., Im, W.J, Kim, S.H., Park, K., Jeong, E.J., Nam, S.Y., et al. (2020) Safety assessment of cerium oxide nanoparticles: Combined repeated-dose toxicity

with reproductive/developmental toxicity screening and biodistribution in rats. *Nanotoxicology,* **14**, 696–710.

Liu, K., Xu, S., Xuan, W., Ling, T., Cao, Z., Huang, B., Sun, Y., Fang, L., Liu, Z., Zhao, N., Shen, W. (2007) Carbon monoxide counteracts the inhibition of seed germination and alleviates oxidative damage caused by salt stress in Oryza sativa. *Plant Science,* **172**, 544–555.

Liu, Q., Chen, Z., Chen, Y., Yang, F., Yao, W., Xie, Y. (2021) Microplastics and nanoplastics: emerging contaminants in food. *Journal of Agricultural and Food Chemistry,* **69**, 10450–10468. 10.1021/acs.jafc.1c04199.

Lopez-Moreno, M.L., de la Rosa, G., Hern´ andez-Viezcas, J.A., Castillo-Michel, H., Botez, C.E., Peralta-Videa, J.R., Gardea-Torresdey, J.L. (2010) Evidence of the differential biotransformation and genotoxicity of ZnO and CeO_2 nanoparticles on *soybean* (*Glycine max*) plants. *Environmental Science & Technology,* **44**, 7315–7320.

Lotfi, N., Vahdati, K., Hassani, D., Kholdebarin, B. (2010) Peroxidase, guaiacol peroxidase and ascorbate peroxidase activity accumulation in leaves and roots of walnut trees in response to drought stress. (April). Available at: *Acta Horticulture* https://doi.org/10.17660/ActaHortic.2010.861.42.

Luo, H., Li, H., Zhang, X., Fu, J. (2011) Antioxidant responses and gene expression in perennial ryegrass (*Lolium perenne* L.) under cadmium stress. *Ecotoxicology,* **20**, 770–778.

Ma, Y., Kuang, L., He, X., Bai, W., Ding, Y., Zhang, Z., Zhao, Y., Chai, Z. (2010) Effects of rare earth oxide nanoparticles on root elongation of plants. *Chemosphere*, **78**(3), 273–279.

Ma, X., Wang, Q., Rossi, L., Zhang, W. (2015) Cerium oxide nanoparticles and bulk Cerium oxide leading to different physiological and biochemical responses in *Brassica rapa*. *Environmental Science and Technology,* **50**(13), 6793-6802.

Mali, M., Aery, N.C. (2009) Effect of silicon on growth, biochemical constituents and mineral nutrition of cowpea *(Vigna unguiculata* L. Walp.). *Community Soil Science and Plant Annals,* **40**, 1041–1052.

Mao, R., Pretti, E., Mittal, J. (2021) Temperature-controlled reconfigurable nanoparticle binary superlattices. *ACS Nano*, **15**(5), 8466-8473.

Maoka, T. (2020) Carotenoids as natural functional pigments. *Journal of Natural Medicines,* **74**(1), 1-16. doi: 10.1007/s11418-019-01364-x.

Mohammadi, M.H.Z., Panahirad, S., Navai, A., Bahrami, M.K., Kulak, M., Gohari, G. (2021) Cerium oxide nanoparticles (CeO_2-NPs) improve growth parameters and antioxidant defense system in Moldavian Balm (*Dracocephalum moldavica* L.) under salinity stress. *Plant Stress*, (1) 100006. https://doi.org/10.1016/j.stress.2021.100006.

Oberoi, H.S., Sandhu, S.K. (2015) Therapeutic and Nutraceutical Potential of Bioactive Compounds Extracted from Fruit Residues AU—Babbar, Neha. Crit. Rev. *Food Science & Nutrition,* **55**, 319–337.

Prakash, V., Peralta-Videa, J., Tripathi, D.K., Ma, X., Sharma, S. (2021) Recent insights into the impact, fate and transport of cerium oxide nanoparticles in the plant-soil continuum. *Ecotoxicology and Environmental Safety,* **221**, 112403. doi: 10.1016/j.ecoenv.2021.112403.

Priester, J.H., Ge, Y., Mielke, R.E., Horst, A.M., Moritz, S.C., Espinosa, K., et al. (2012) Soybean susceptibility to manufactured nanomaterials with evidence for food quality and soil fertility interruption, *Proc. Natl. Acad. Sci.* 109, 2451–2456.

Panda, S.K., Matsumoto, H. (2010) Changes in antioxidant gene expression and induction of oxidative stress in pea *(Pisum sativum* L.) under Al stress. *Biometals,* **23**, 753–762.

Pollard, M., Beisson, F., Li, Y., Ohlrogge, J.B. (2008) Building lipid barriers: biosynthesis of cutin and suberin. *Trends in Plant Science,* **13**, 236–246.

Pullagurala, V.L. R., Adisa, I.O., Rawat, S., Kalagara, S., Hernandez-Viezcas, J.A., Peralta-Videa, J.R., Gardea-Torresdey, J.L. (2018) ZnO nanoparticles increase photosynthetic pigments and decrease lipid peroxidation in soil grown cilantro (*Coriandrum sativum*). *Plant Physiology and Biochemistry*, **132**, 120-127.

Racchi, M. (2013) Antioxidant defenses in plants with attention to Prunus and Citrus Spp. *Antioxidants,* **2**, 340-369.

Rafael, J., Julio, M., Manzaneda, J., Rey Pedro, J. (2018) Climate change decreases suitable areas for rapeseed cultivation in Europe but provides new opportunities for white mustard as an alternative oilseed for biofuel production . *PLOS ONE*. **13**(11), e0207124. doi:10.1371/journal.pone.0207124.

Ramaye, Y., Dabrio, M., Roebben, G., Kestens, V., (2021) Development and validation of optical methods for zeta potential determination of silica and polystyrene particles in aqueous Suspensions. *Materials,* 14(2), 290. https://doi.org/10.3390/ma14020290.

Ramel, F., Sulmon, C., Bogard, M., Couée, I., Gouesbet, G. (2009) Differential patterns of reactive oxygen species and antioxidative mechanisms during atrazine injury and sucrose-induced tolerance in *Arabidopsis thaliana* plantlets. *BMC Plant Biology,* **9**(28), 220–228.

Rico, C.M., Morales, M.I., McCreary, R., Castillo-Michel, H., Barrios, A.C., Hong, J., et al., (2013) Cerium oxide nanoparticles modify the antioxidative stress enzyme activities and macromolecule composition in rice seedlings. *Environmental Science and Technology,* **47**, 14110–14118.

Rossi, L., Zhang, W., Ma, X. (2017) Cerium oxide nanoparticles alter the salt stress tolerance of *Brassica napus* L. by modifying the formation of root apoplastic barriers. *Environmental Pollution,* **229**, 132–8. doi : 10.1016/j.envpol.2017.05.083.

Salehi, H., Chehregani Rad, A., Raza, A. (2021) Chen. foliar application of CeO_2 nanoparticles alters generative components fitness and seed productivity in Bean crop (*Phaseolus vulgaris* L.), *Nanomaterials,* **11**, 862. doi: 10.3390/nano11040862.

Sahoo, S., Maiti, M., Ganguly, A., Jacob George, J. Bhowmick, A.K. (2007) Effect of zinc oxide nanoparticles as cure activator on the properties of natural rubber and nitrile rubber. *Journal of Applied Polymer Science,* **105**, 2407–2415. 10.1002/app.26296.

Safi, A., Numan, M., Khan, A. L., Imran, M. (2020) Melatonin : Awakening the defense mechanisms during plant oxidative stress melatonin: Awakening the defense mechanisms during plant oxidative stress. March. https://doi.org/10.3390/plants9040407.

Shen, C., Zhang, Q., Li, J., Bi, F., Yao, N. (2010) Induction of programmed cell death in Arabidopsis and rice by single- wall carbon nanotubes. *American Journal of Botany*, **97**(10), 1620-1609.

Singh, S., Husen, A. (2019) Role of nanomaterials in the mitigation of abiotic stress in plants. In: "*Nanomaterials & Plant Potential*", Husen A., Iqbal, M. (Eds.). Springer; Cham, Switzerland. pp. 441–471.

Singh, S., Dosani, T., Karakoti, A.S., Kumar, A., Seal, S., Self, W.T. (2011) A phosphate-dependent shift in redox state of cerium oxide nanoparticles and its effects on catalytic properties. *Biomaterials*, **32**, 6745–6753.

Sohail, L.E., Ferrari, Stierhof Y.D., Kemmerling, B., Mashwani, Z.U. (2022) Molecular effects of biogenic zinc nanoparticles on the growth and development of *Brassica napus* L. revealed by proteomics and transcriptomics. *Frontiers in Plant Science*, **13**, 798751.doi: 10.3389/fpls.2022.798751.

Sun, L., Yan, X.L., Liao, X.Y., Wen, Y., Chong, Z.Y., Liang, T. (2011) Interactions of arsenic and phenanthrene on their uptake and antioxidative response in Pteris vittata L. *Environmental Pollution,* **159**, 3398–3405.

Thomas, P.J., Carpenter, D., Boutin, C., Allison, J.E. (2014) Rare earth elements (REEs): effects on germination and growth of selected crop and native plant species. *Chemosphere,* **96**, 57–66.

Tombuloglu, H., Semizoglu, N., Sakcali, S., Kekec, G. (2012) Boron induced expression of some stress-related genes in tomato. *Chemosphere,* **86**, 433–438.

Tiseanu, C., Parvulescu, V.I., Boutonnet, M., Cojocaru, B., Primus, P.A, Teodorescu, C.M., Solans, C., Sanchez Dominguez, M. (2011) Surface versus volume effects in luminescent ceria nanocrystals synthesized by an oil-in-water microemulsion method. *Physical Chemistry Chemical Physics,* **13**, 17135–17145.

Wang, Q., Ebbs, S.D., Chen, Y., Ma, X. (2013) Trans-generational impact of cerium oxide nanoparticles on tomato plants *Metallomics,* **5**, 753–759. doi: 10.1039/c3mt00033h.

Wu, X., He, J., Zhu, Z., Yang, S., Zha, D. (2014) Protection of photosynthesis and antioxidative system by 24-epibrassinolide in *Solanum melongena* under cold stress. *Biologia Plantarum,* **58**, 185–188.

Wu, H., Tito, N., Giraldo, J.P. (2017) Anionic cerium oxide nanoparticles protect plant photosynthesis from abiotic stress by scavenging reactive oxygen species. *ACS Nano,* **11**, 11283–11297.

Yu, Q., Wang, Z., Zhai, Y., Zhang, F., Vijver, M.G., Peijnenburg, W.J.G.M. (2021) Effects of humic substances on the aqueous stability of cerium dioxide nanoparticles and their toxicity to aquatic organisms. *Science of the Total Environment,* **10**, 781:146583. doi: 10.1016/j.scitotenv.2021.146583.

Yuan, S., Wu, Y., Cosgrove, D.J. (2001) A fungal endoglucanase with plant cell wall extension activity. *Plant Physiology,* **127**(1), 324–333.

Zaman, S., Hu, S., Alam, M.A., Du, H., Che, S. (2019) The accumulation of fatty acids in different organs of purslane under salt stress. *Scientia Horticulturae,* **250**, 236–242 doi: 10.1016/j.scienta.2019.02.051.

Zhao, L., Peng, B., Hernandez-Viezcas, J.A., Rico, C., Sun, Y., Peralta-Videa, J.R., Zhang, J.Y., (2012) Stress response and tolerance of Zea mays to CeO2 nanoparticles: cross talk among H_2O_2, heat shock protein, and lipid peroxidation. *ACS Nano*, **6**, 9615–9622.

Zhang, W.F., Zhang, F., Raziuddin, R., Gong, H.J., Yang, Z.M., Lu, L., Ye, Q.F., Zhou, W.J. (2008) Effects of 5-aminolevulinic acid on oilseed rape seedling growth under herbicide toxicity stress. *Journal of Plant Growth Regulation,* **27**, 159–169.

Zhou, W.J., Leul, M. (1999) Uniconazole-induced tolerance of rape plants to heat stress in relation to changes in hormonal levels, enzyme activities and lipid peroxidation. *Plant Growth Regulation,* **27**, 99–104.

الأدوار المتعددة لجسيمات أكسيد السيريوم النانوية المُصنَّعة حيوياً علي المعايير المورفولوجية والفسيولوجية والجزيئية لنبات الكانولا

سلمى محمد عوض[1]، تهانى عباس حتحوت[1]، سامية محب الخلال[1]، خالد يحي فروح[2]

[1]قسم النبات - كلية البنات - الآداب والعلوم والتربية- جامعة عين شمس- القاهرة 11757 -مصر، [2] المعمل المركزي لتكنولوجيا النانو والمواد المتقدمة (NAMCL) - مركز البحوث الزراعية- الجيزة- مصر.

يهدف هذا البحث إلى دراسة كيفية تأثير جزيئات ثاني أكسيد السيريوم النانوية على التغييرات ف معايير النمو والفسيولوجي لنبات الكانولا. تم تصنيع جزيئات ثاني أكسيد السيريوم النانوية حيويًا باستخدام مستخلص الصبار وتم تميزها باستخدام مقياس الطيف الضوئي المرئي للأشعة فوق البنفسجية، وانحراف الأشعة السينية، والتحليل الطيفي للأشعة تحت الحمراء لتحويل فورييه، وإمكانات زيتا وحجم الجسيمات بالإضافة إلى المجهر الإلكتروني. وتمت رش اوراق النبات بتركيزات 250 و 500 و 1000 جزء في المليون من جزيئات ثاني أكسيد السيريوم النانوية، وتم تقييم تقيمم تأثيره علي النبات. وأدى التعرض لـ 500 جزء في المليون من جزيئات ثاني أكسيد السيريوم النانوية إلى تعزيز الخصائص المورفولوجية والنمو والأيض ومن ثم الإنزيمات المضادة للأكسدة ومحتوى الفينول وتوكوفيرول ومحتوى الكلوروفيل بالإضافة إلى مستويات الكاروتينات في البراسيكا نابس. كما تم تقييم معاملات بيروكسيد الدهون عند استخدام التركيزات المحضرة لـ جزيئات ثاني أكسيد السيريوم النانوية التي تعكس تأثير جزيئات ثاني أكسيد السيريوم النانوية في التنظيم السفلي لكمية MDA وجذر الأنيون الفائق الكمي ($O_2^{\cdot -}$) بالإضافة إلى التنظيم الكمي لبيروكسيد الهيدروجين والتنظيم السلبي لإنزيم وLipoxygenase. يؤكد الرش الكيميائي للنسيج لأوراق براسيكا نابوس باستخدام تترازوليوم النيترو الأزرق دور رش 500 جزء في المليون من CeO_2 NPs في تراكم الجزيئات المؤكسدة في الأوراق. وأبرز اختبار التعبير الجيني لـ SOD و MT دور جزيئات ثاني أكسيد السيريوم النانوية في تنظيم الجينات المرتبطة بالإجهاد في النباتات المختبرة. فحص البنية التحتية الفحص بالميكرسكوب الالكترونى لأوراق براسيكا نابوس المعالجة بـ 500 جزء في المليون من جزيئات ثاني أكسيد السيريوم النانوية بالمقارنة إلى المجموعة العادية الغير معاملة.